Contents lists available at ScienceDirect

Engineering Applications of Artificial Intelligence

journal homepage: www.elsevier.com/locate/engappai

Research paper

Enabling temporal–spectral decoding in multi-class single-side upper limb classification

Hao Jia [a], Shuning Han [a], Cesar F. Caiafa [b], Feng Duan [c], Yu Zhang [d], Zhe Sun [e], Jordi Solé-Casals [a,f,*]

[a] Data and Signal Processing Research Group, Department of Engineering, University of Vic–Central University of Catalonia, Vic, 08500, Spain
[b] Instituto Argentino de Radioastronomía, CONICET CCT La Plata/CIC-PBA/UNLP, V. Elisa, 1894, Argentina
[c] Tianjin Key Laboratory of Brain Science and Intelligent Rehabilitation, College of Artificial Intelligence, Nankai University, Tianjin, 300110, China
[d] Department of Bioengineering and Department of Electrical and Computer Engineering, Lehigh University, Bethlehem, PA 18015, USA
[e] Faculty of Health Data Science, Juntendo University, Urayasu, Chiba, Japan
[f] Department of Psychiatry, University of Cambridge, Cambridge, United Kingdom

ARTICLE INFO

ABSTRACT

This manuscript presents a novel approach for decoding pre-movement patterns from brain signals using a two-stage-training temporal–spectral neural network (TTSNet). The TTSNet employs a combination of filter bank task-related component analysis (FBTRCA) and convolutional neural network (CNN) techniques to enhance the classification of single-upper limb movements in non-invasive brain–computer interfaces (BCIs).

In our previous work, we introduced the FBTRCA method which utilized filter banks and spatial filters to handle spectral and spatial information, respectively. However, we observed limitations in the temporal decoding phase, where correlation features failed to effectively utilize temporal information because of misaligned onset and noisy spikes. To address this issue, our proposed method focuses on analyzing multi-channel signals in the temporal–spectral domain. The TTSNet first divides the signals into various filter banks, employing task-related component analysis to reduce dimensionality and eliminate noise, respectively. Subsequently, a CNN is employed to optimize the temporal characteristics of the signals and extract class-related features. Finally, the class-related features from all filter banks are concatenated and classified using the fully connected layer.

To evaluate the effectiveness of our proposed method, we conducted experiments on two publicly available datasets. In binary classification tasks, the TTSNet achieved an improved accuracy of 0.7707 ± 0.1168, surpassing the performance of EEGNet (accuracy: 0.7340 ± 0.1246) and FBTRCA (accuracy: 0.7487 ± 0.1250). In multi-class tasks, TTSNet achieved an accuracy of 0.4588 ± 0.0724, exhibiting a 4.27% and 3.95% accuracy increase over EEGNet and FBTRCA, respectively.

The findings of this study suggest that the proposed TTSNet method holds promise for detecting limb movements and assisting in the rehabilitation of stroke patients. The classification of single-side limb movements is expected to facilitate the interaction between patients and external environment by increasing the number of control commands in BCIs.

1. Introduction

Non-invasive brain–computer interfaces (BCIs) serve as a link between the human brain and external devices, such as computers and robots (Hramov et al., 2021; Saha et al., 2021; Kawala-Sterniuk et al., 2021). They enable the conversion of brain activity into control commands by analyzing electroencephalogram (EEG) data. The EEG signals are non-invasively acquired from the scalp using specialized acquisition devices.

Movement-related cortical potential (MRCP) is a brain activity associated with single-side upper limb movement (Olsen et al., 2018; Ofner et al., 2017, 2019; Farina et al., 2013; Ghani et al., 2023). When a subject's limb moves, EEG signals acquired from the motor cortex show an increase in amplitude in the low-frequency domain Ofner et al. (2017, 2019). Due to noise influences during signal acquisition, the EEG signals are averaged across multiple trials of repeated motions to reduce

the noise impact. The averaged signal across multiple trials belonging to same motion, known as the grand average MRCP, is used to reduce the impact of noise during signal acquisition (Borràs et al., 2022). Distinct differences in the grand average MRCPs are observed before and after movement onset when different upper limb motions, such as hand closure and elbow flexion, are executed (Ofner et al., 2017). These differences in grand average MRCPs serve as discriminative features for classifying the upper limb movements of subjects.

Previous studies on MRCP signals have focused on two tasks: movement detection and movement classification (Kaeseler et al., 2022). Movement detection aims to distinguish between movement and resting states, representing a binary classification task. In contrast, movement classification involves distinguishing between binary or multi-class movement states. During movement states, the grand average MRCP exhibits fluctuations characterized by an initial increase followed by a subsequent decrease around the movement onset. In contrast, the grand average MRCP during the resting state remains relatively stable in comparison to the movement state (Ofner et al., 2017). It is worth noting that movement detection, which classifies signals as fluctuating or steady, generally achieves higher classification accuracy compared to movement classification, as it represents a subset of the broader movement classification task.

The movement detection problem is tackled using the subject-dependent and section-wise spectral filtering method, which considers MRCP signals in two different temporal sections (Jeong et al., 2020). These sections comprise a two-second time window before the movement onset and a one-second time window after the movement onset. The signals within each section are averaged, and the mean amplitudes in both sections are used as features, which are subsequently fed into a regularized linear discriminant analysis classifier. This method utilizes the changes in amplitude of MRCP signals before and after the movement onset. However, the signal averaging approach overlooks the temporal dynamics of amplitude changes, potentially leading to information loss during signal processing.

EEG source imaging is another valuable contribution to the classification of single-side limb movement (Edelman et al., 2016). Instead of directly analyzing brain images, this technique initially identifies the region of interest. Following this, the EEG signals within the identified region of interest are analyzed in the time–frequency domain.

In our previous work, we proposed the standard task-related component analysis method (STRCA) to address the movement detection problem (Duan et al., 2021). This method utilizes task-related component analysis (TRCA) as a spatial filter to remove noise and task-unrelated components from EEG signals. The spatial filtering process can be seen as a method for identifying the regions of interest. This spatial filter is also mentioned in the decoding of continuous finger movements to process MRCP signals (Liu et al., 2023). After applying spatial filtering to both the unlabeled signals and the grand average MRCPs, canonical correlation coefficients are calculated to measure the similarity between the unlabeled signals and multiple grand average MRCPs. The extracted coefficients are then used as features for linear discriminant analysis (LDA) classifier, which classifies the signals and predicts their labels. To capture information about the amplitude changes in MRCP signals, STRCA compares the unlabeled signals with the grand average MRCPs and uses the calculated similarity as a feature.

Frequency domain analysis is a widely used approach for analyzing time series data. To harness information across various frequencies, we introduced the filter bank task-related component analysis method (FBTRCA) (Jia et al., 2022). The EEG signals are divided into multiple filter banks, with a consistent low cut-off frequency of 0.5 Hz. The high cut-off frequencies are arranged in an arithmetic sequence ranging from 1 Hz to 10 Hz. STRCA is used to extract features from each filter bank, and the resulting features are concatenated. For feature selection, we use a method based on mutual information, *i.e.*, minimum redundancy maximum relevance (mRMR) to select the most informative features.

Finally, the selected features are classified using a support vector machine (SVM) classifier.

In STRCA, the spatial filter is derived by concatenating the task-related component analysis spatial filters of two classes. However, as the number of classes increases, the number of vectors along the concatenation axis exceeds the number of EEG channels. This limitation restricts the use of STRCA and FBTRCA in multi-class tasks. To address this limitation and enable the use of STRCA and FBTRCA in multi-class classification, we optimized the structure of the spatial filter and eliminated the common component from the grand average MRCPs. The common component is obtained by averaging the grand average MRCPs of multiple classes. This modification allows for the application of FBTRCA in both movement detection and classification tasks (Jia et al., 2023).

Analyzing EEG signals in the time domain provides valuable insights. For instance, in motor imagery tasks, employing sliding time windows enhances the classification performance between movements of the left and right limbs. A deep learning method named EEGNet has proven to be an effective tool for processing EEG signals (Lawhern et al., 2018). EEGNet is capable of leveraging the temporal information within EEG signals due to its shift-invariant properties in the convolutional layers.

Our previously proposed method, FBTRCA, leverages information from various filter banks. In FBTRCA, temporal information is evaluated using a simple correlation measure between unlabeled EEG signals and the grand average MRCPs. This correlation heavily relies on the grand average MRCPs, which can be susceptible to noise. While noise in the grand average MRCPs is reduced through signal averaging within the same class, it is important to note that the grand average MRCPs utilized in FBTRCA may still be affected by unknown noise sources such as spikes. Furthermore, in scenarios where the precise localization of movement onset is challenging, there may be latency differences between the MRCP signals of two trials (Sburlea et al., 2015).

In this work, our objective is to enhance the temporal decoding of FBTRCA and improve its performance. To achieve this, we introduce a two-stage-training temporal–spectral neural network (TTSNet). TTSNet incorporates the shift-invariant properties of convolutional layers and integrates temporal information into the FBTRCA method. The TTSNet model comprises four steps: (1) dividing EEG signals into filter banks, (2) optimizing the EEG signals using the spatial filter, (3) extracting temporal features using EEGNet, and (4) concatenating the extracted features and performing classification using a fully connected layer.

The structure of this work is organized as follows. Section 2 introduces the EEG datasets utilized in this study and describes the preprocessing steps applied to these datasets. Additionally, it presents the detailed structure of the proposed method. Section 3 evaluates the classification performance of the proposed method on the EEG dataset and compares it against other state-of-the-art methods. Section 4 explains the design of the proposed method and how it utilizes information from the grand average MRCP. Finally, Section 5 provides the concluding remarks for this paper.

2. Material and methods

2.1. Dataset description

In this work, we evaluate the classification performance using two public datasets pertaining to upper limb movement, namely Dataset I and Dataset II. Dataset I comprises EEG data from 15 healthy subjects (Ofner et al., 2017), while Dataset II contains EEG data from 10 subjects with cervical spinal cord injuries (Ofner et al., 2019). The preprocessing of the raw EEG signals in this study follows the same procedures as detailed in our previous works.

Each subject was seated in front of a computer with their arm supported by a table or exoskeleton to minimize muscle fatigue. The signal acquisition paradigm employed in this study followed a trial-based
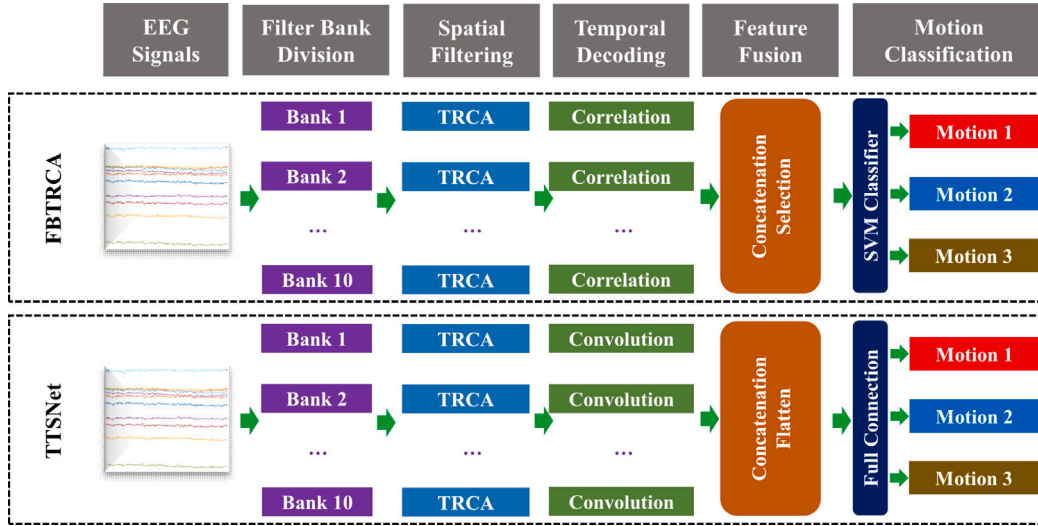
Fig. 1. The overall framework of the multi-class FBTRCA method and the TTSNet method. In both methods, EEG signals are divided into filter banks and then optimized with the spatial filter TRCA. During the decoding of temporal information from signals, FBTRCA uses the correlation between these signals and the grand average MRCPs as the features. TTSNet uses the EEGNet to capture the temporal information and use the shift-invariant of the convolution layers. Following the decoding of temporal information, output features from all filter banks are concatenated. In FBTRCA, these features are selected and optimized by the mRMR method and classified by the SVM method. In TTSNet, these features are flattened and subsequently classified by the fully connected layer.

approach, with each trial lasting 5 s. At 0 s, the trial commenced with an auditory beep, accompanied by a cross displayed on the computer screen. Two seconds later, a cue was presented on the screen, indicating the required movement to be executed by the subject.

Dataset I consists of movements including *elbow flexion, elbow extension, supination, pronation, hand close, hand open,* and *resting.* In dataset II, the executed movements include *supination, pronation, hand open, palmar grasp,* and *lateral grasp.* Dataset I comprises 60 trials per class, whereas dataset II consists of 72 trials per class.

In dataset I, the movement trajectories of the hand were simultaneously recorded by the exoskeleton during the EEG signal acquisition, allowing for the accurate localization of the movement onset. However, in dataset II, the movement trajectories were not recorded, and thus, the movement onset for each trial is unknown. Additionally, the latency lag between the movement onset and the cue cannot be eliminated in dataset II. To investigate the influence of movement onset on the classification performance, we divide the experiments conducted on dataset I into two cases: dataset I(a) and dataset I(b). In dataset I(a), the recorded movement trajectories are used to locate the movement onset. The EEG signals recorded from one second before the movement onset to one second after the movement onset are used in the evaluation and classification tasks. In dataset I(b), the assumption is made that the movement trajectories were not recorded, making it impossible to reject contaminated trials or accurately locate the movement onset. Consequently, the EEG signals used in the classification task extend from the cue to two seconds after the cue. Similarly, in dataset II, the range of EEG signals used for classification consists of a two-second time window following the cue.

Because dataset I has the simultaneously acquired hand trajectories, but dataset II does not, the movement onset can be located with the trajectories in dataset I. In the localization of the movement onset in dataset I, the 1-order difference of the trajectory is first smoothed by the 1-order *Savitzky–Golay* finite impulse response smoothing filter with time window length 31. The filtered 1-order difference is then normalized by the maximum absolute value. For trials belonging to the *resting* state, a fake movement onset is set to 2.5 s after the trial starts. Trials in the *resting* state are rejected if the variances of normalized trajectory are less than 0.02. In *elbow flexion* and *elbow extension,* the amplitude of the hand trajectory is higher than the other four motions because the limb moves. The movement onset is set to the location where the normalized trajectory equals the threshold of 0.05. Trials are

rejected manually when the movement onset is highly influenced by noise contamination. In the other four motions, the function $f(x) = a * exp(-(\frac{x-b}{c})^2) + d$ is used to fit the smoothed and normalized trajectory by tuning the parameters a, b, c, d (Duan et al., 2021; Jia et al., 2022). Trials are rejected if the parameters of the tuned function fulfill $a < 0.05$, $c > 100$, and $d > 10$. The movement onset is set to the time point whose absolute amplitude equals 0.1.

The EEG signals for classification were acquired from the motor cortex of the brain, namely FC_z, C_3, C_z, C_4, CP_z, F_3, F_z, F_4, P_3, P_z and P_4. The raw EEG signals are firstly downsampled to 256 Hz. The z-normalization is then used to normalize the EEG signals. Because the MRCP signals are located at the low-frequency bands of EEG signals, the normalized EEG signals are bandpassed to 0.5~10 Hz.

2.2. Two-stage-training temporal-spectral network

The two-stage-training temporal–spectral network (TTSNet) is further developed based on the FBTRCA method and has four steps: (1) filter bank division, (2) spatial filtering, (3) temporal decoding, and (4) feature fusion and classification. The overall framework of both the FBTRCA and TTSNet is given in Fig. 1, which shows the relationship and the differences between the two methods.

2.2.1. Filter bank division

The MRCP signals are located at the low-frequency bands of EEG signals. The approximate range of the low-frequency bands is 0.5~10 Hz. To use the information in the frequency domain of MRCP signals, we proposed a filter bank division method for the low-frequency bands. The low cut-offs of these bands are fixed at 0.5 Hz. The high cut-offs of these bands are sorted as an arithmetic sequence from 1 Hz to 10 Hz with step 1 Hz. Therefore, the range of the low-frequency bands, 0.5~10 Hz, is divided into F filter banks, where $F = 10$.

2.2.2. Spatial filtering

After the filter bank division, the MRCP signals are divided into various filter banks. In each filter bank, the multi-channel signals contain task-unrelated components because the filter bank division cannot remove the noise from the original signals. Here, we use the spatial filter to reject the noise and remove task-unrelated components from the original signals in each filter bank. A spatial filter is a matrix W with size $C \times P$, where C is the number of channels and P is an
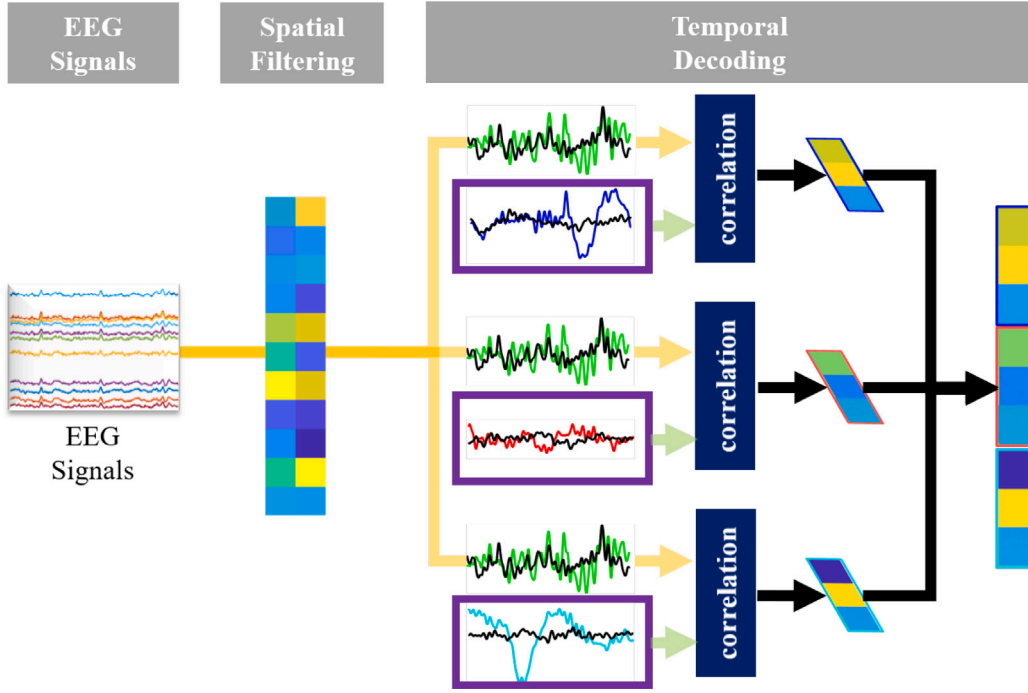
Fig. 2. The structure of the temporal decoding component from one filter bank in the FBTRCA method. The EEG signals undergo initial filtering using the spatial filter TRCA to remove unrelated noise and reduce signal dimensions. To capture the amplitude changes of the filtered signals, the correlation between the filtered signals and the corresponding filtered grand average MRCPs (shown in the purple box) of their respective classes is computed as the features. These correlation features from all classes are concatenated to form the output features.

integer smaller than C. Spatial filtering is the operation that multiplies the spatial filter and the raw EEG signals. By the matrix multiplication between the original signals $X \in \mathbb{R}^{C \times T}$ and the W, the spatial-filtered signals $X^T W \in \mathbb{R}^{T \times P}$ has a decreased dimension, and the noise is removed. Here, TRCA is used as the spatial filter, which aims to find a W that maximizes the inter-trial covariances within a class. The training set belonging to the class k is $\mathcal{X}^k = \{X_1, X_2, \ldots, X_N\}$, where N is the number of trials of class k and $X_N \in \mathbb{R}^{C \times T}$. The inter-trial covariance of class k is computed with the equation:

$$S^k = \sum_{i,j=1,i<j}^{N} X_i^T X_j + X_j^T X_i. \tag{1}$$

To normalize the inter-trial covariance, the self-covariance is introduced:

$$Q^k = \sum_{i=1}^{N} X_i^T X_i. \tag{2}$$

The spatial filter TRCA is obtained by solving the Eigen equation:

$$J = \max_{\omega} \frac{\omega^T S \omega}{\omega^T Q \omega} \tag{3}$$

where $\omega \in \mathcal{R}^{C \times 1}$ is the eigenvector. S and Q are the matrices that summarized the inter-covariances and self-covariances of K classes:

$$S = \sum_{k=1}^{K} S^k, Q = \sum_{k=1}^{K} Q^k. \tag{4}$$

The eigenvectors ω of maximum eigenvalues are concatenated into the spatial filter $W \in \mathbb{R}^{C \times P}$, where P is the number of selected eigenvectors.

2.2.3. Temporal decoding
Temporal decoding serves as a feature extraction mechanism in both FBTRCA and TTSNet. In FBTRCA, the correlated coefficient is utilized as a feature to quantify the dissimilarities between the unlabeled EEG signals and the grand average MRCPs. However, the correlation

coefficient can only capture stationary temporal characteristics and cannot effectively handle shifted temporal characteristics. Therefore, we propose TTSNet, which enhances the temporal decoding capability of FBTRCA by incorporating a convolutional neural network (CNN).

Correlation coefficient. The correlation coefficient measures the similarity of two matrices. In FBTRCA, the two input matrices are the spatial-filtered unlabeled signals and the spatial-filtered grand average MRCPs. In Fig. 2, the structure for computing correlation coefficients in FBTRCA is depicted.

The grand average MRCP of class k is obtained from the training set $\mathcal{X}^k$ by taking the average of all trials:

$$\hat{X}^k = \frac{1}{N} \sum_{i=1}^{N} X_i \tag{5}$$

The averaged signals of the grand average MRCPs of K classes is firstly removed from both the grand average MRCPs $\hat{X}^k$ and the unlabeled signals $X \in \mathbb{R}^{C \times T}$:

$$\hat{X}_{\&}^k = \hat{X}^k - \frac{1}{K} \sum_{k=1}^{K} \hat{X}^k, X_{\&} = X - \frac{1}{K} \sum_{k=1}^{K} \hat{X}^k \tag{6}$$

The correlation coefficient is a normalized point-wise product of two input matrices. Given two input matrices $X, Y \in \mathbb{R}^{I \times J}$ that fulfill $mean(X) = 0$ and $mean(Y) = 0$, the correlation coefficient is computed using:

$$r = corr(X, Y) = \frac{X * Y}{\sqrt{(X * X) \times (Y * Y)}} \tag{7}$$

where $*$ denotes the summed-up point-wise products of two input matrices. The symbol $\times$ multiplies two constants $(X * X)$ and $(Y * Y)$.

Three correlation coefficients are computed by taking $X_* = X_{\&}^T W$ and $X_k = \hat{X}_{\&}^k{}^T W$ as the inputs.

(1) Correlation Coefficient

$$\rho_{1,k} = corr(X_*, X_k); \tag{8}$$

Table 1
The model structure of temporal decoding in TTSNet.

Layer	Output size	Parameter
Input layer	$[B, 1, C, T]$	
ZeroPad2d	$[B, 1, C, T + 63]$	$(31, 32, 0, 0)$
Conv2d	$[B, 8, C, T]$	$(1, 64)$
BatchNorm2d	$[B, 8, C, T]$	
Conv2d	$[B, 16, 1, T]$	$(C, 1),\ grouped$
BatchNorm2d	$[B, 16, 1, T]$	
ELU	$[B, 16, 1, T]$	
AvgPool2d	$[B, 16, 1, T//4]$	$(1, 4)$
Dropout	$[B, 16, 1, T//4]$	0.25
ZeroPad2d	$[B, 16, 1, T//4 + 15]$	$(7, 8, 0, 0)$
Conv2d	$[B, 16, 1, T//4]$	$(1, 15),\ grouped$
Conv2d	$[B, 16, 1, T//4]$	$(1, 1)$
BatchNorm2d	$[B, 16, 1, T//4]$	
ELU	$[B, 16, 1, T//4]$	
AvgPool2d	$[B, 16, 1, T//32]$	$(1, 8)$
Dropout	$[B, 16, 1, T//32]$	0.25
Flatten	$[B, 16*T//32]$	
Linear	$[B, K]$	$bias = False$

Table 2
The model structure of classification in TTSNet.

Layer	Output size	Parameter
Input layer	$[B, K, F]$	
Flatten	$[B, K * F]$	
Linear	$[B, K * F * 2]$	$bias = False$
Relu	$[B, K * F * 2]$	
Linear	$[B, K * F//2]$	$bias = False$
Relu	$[B, K * F//2]$	
Linear	$[B, K]$	$bias = False$

(2) Canonical Correlation Coefficient

$$[A, B] = cca(X_*, X_k) \tag{9}$$

$$\rho_{2,k} = corr(X_*B, X_kB); \tag{10}$$

(3) Normalized Canonical Correlation Coefficient

$$[A, B] = cca(X_* - X_k, X_{-k} - X_k) \tag{11}$$

$$\rho_{3,k} = corr((X_* - X_k)A, (X_{-k} - X_k)A); \tag{12}$$

where X_{-k} is the mean of the spatial-filtered grand average MRCPs of all classes except for class K:

$$X_{-k} = \frac{1}{K - 1} \sum_{kk=1, kk \neq k}^{K} X_{kk}. \tag{13}$$

Therefore, there are $3 \times K \times F$ features in FBTRCA, where F is the number of filter banks.

Convolution neural network. The correlation coefficients used in FB-TRCA measure the similarity between unlabeled trials and the grand average MRCPs, facilitating the temporal decoding of the signals. The correlation coefficient in Eq. (7) has two inputs. One is the input EEG signal, and the other is the grand average MRCP, which can be viewed as the pre-trained weights obtained by averaging EEG signals across trials in the training set. However, the temporal decoding aspect of FBTRCA requires improvement for two reasons:

(1) The grand average MRCP is obtained by averaging across trials of the same class. Noise cannot be completely removed by averaging, and noise such as spikes will influence the shape of the overall average MRCP obtained. This means that the use of the grand mean MRCP as a weight is not sufficiently robust.

(2) In cases where the movement onset cannot be precisely located or is subject to bias, the MRCP signals may be shifted from the true onset. Correlation alone cannot effectively address the misalignment caused by the shifted onset. The issue of misaligned onsets will be further discussed in Section 4.

The grand average MRCP, serving as the weight applied to the input signals, can be further improved due to its simple derivation through trial averaging. Replacing the role of correlation in temporal decoding, convolutional neural networks (CNNs) offer two advantages: (1) trainable weights and (2) shift-invariant properties. For this purpose, we employ the network architecture of EEGNet in temporal decoding due to its superior classification performance. The specific network architecture is provided in Table 2.

2.2.4. Classification

In FBTRCA, the features of all filter banks are sorted and selected by the mRMR method and then classified by the SVM classifier. The proposed TTSNet uses a fully connected layer to optimize these features and classify the features, whose architecture is given in Table 2.

2.2.5. Two-stage training

The TTSNet has two modules that consist of neural networks, the CNN for temporal decoding and the fully connected layer for classification. During training the TTSNet, the two modules are trained separately, *i.e.*, in a two-stage approach. In the first stage, a CNN will be trained for each of the filter banks, and thus the number of trained CNNs is F. The output of the F CNNs is concatenated and flattened. In the second stage, the fully connected layer is trained with the flattened features from the CNNs. As given in Table 1, the output layer is a linear layer of output size K, where K is the number of classes. Therefore, the network can be trained with the losses between the train label and the outputs. The train label is used twice in the two-stage training process, the temporal decoding in Table 1 and the classification in Table 2. In the first stage, the weights in the fully connected layer are fixed, and the CNNs are trained with train labels. In the second stage, the weights in the CNNs are fixed, and the fully connected layer is trained with train labels.

Summarizing, we can get the training process of the TTSNet. The training of TTSNet consists of two stages. The first stage involves the training of the model parameters within each filter bank, including the spatial filter and the EEGNet. In the second stage, the fully connected layer will be trained.

In the first-stage training process, the following two points should be noted:

- *Decision on spatial filter*: The number of columns (P) of the spatial filters is a hyperparameter. To decide on the hyperparameter, the training set is divided into a sub-training set and a validation set. Then, the accuracy of STRCA is calculated for different values of the hyperparameter P. The best hyperparameter is the one which generates the highest accuracy. With the best hyperparameter, the spatial filter is recalculated for each filter bank with all trials in the training set. The obtained spatial filter will not be changed in the following training steps.
- *Parameter Tuning on EEGNet*: In each filter bank, the EEG signals are optimized by passing through the spatial filter. The filtered signals are used as the input of the EEGNet. With the true labels of the training set, the weights of the EEGNet will be trained. The trained weights of the EEGNets will not be changed in the following training step.

Note that the models (spatial filter and EEGNet) are independent across the filter banks. It means that the spatial filter and the weights of the EEGNet are not the same between two arbitrary filter banks.

In the second stage, the fully connected layer will be trained. The original EEG signals are bandpassed into multiple filter banks. In each filter bank, the model parameters are already trained in the first stage. After applying the trained models to the original signals, the input features of the fully connected layer are obtained. The model parameters of the fully connected layer are finally trained.

2.3. Compared methods

In our previous work (Jia et al., 2023), the FBTRCA method was compared against both machine learning methods and deep learning methods, such as multi-class common spatial pattern (Grosse-Wentrup and Buss, 2008), minimum distance to mean (Barachant et al., 2012), WaveNet (Thuwajit et al., 2022), and Deep CNN (Schirrmeister et al., 2017). The methods based on common spatial pattern have a worse performance than FBTRCA in the decoding of single-side upper limb movement. The methods for comparison in this work have two state-of-the-art methods (FBTRCA, EEGNet) and three baseline methods.

Baseline I: TEGNet Compared to the EEGNet, The TTSNet fuses the temporal features from all filter banks. To bridge the gap between TTSNet and EEGNet in the comparison, we additionally introduce the Tasked-related EEGNet (TEGNet). The TEGNet consists of the spatial filter TRCA and the EEGNet, which processes only signals from one filter bank.

Baseline II, OTSNet The TTSNet is trained in two steps. To show the necessity of the two-stage training, the performance of TTSNet is compared to the one-stage-training temporal–spectral neural network (OTSNet). In OTSNet, the EEGNet and the fully connected layer are trained simultaneously.

Baseline III, TTSSVM In TTSNet, two modifications have been made to FBTRCA, the temporal decoding with EEGNet and the classification with the fully connected layer. To observe the effects of the two modifications, the fully connected layer is replaced with the SVM classifier, which is used in FBTRCA.

3. Result analysis

3.1. Parameter setting

The classification tasks in this experiment include (1) the binary classification between two motions, *e.g.*, *elbow flexion* and *elbow extension*, and (2) the multi-class classification among all the motions in each dataset. In both classification tasks, the two datasets are split into the training set and the testing set by ten-fold cross-validation. The mean and standard deviation of the accuracy of ten folds are used to evaluate the performance of the mentioned classification methods. A two-sample t-test is also used to measure the statistical significance of the improvement between the proposed method and the compared methods.

The training process of EEGNet, TEGNet, OTSNet, and TTSNet all has the parameters: learning rate (0.001), batch size (50), optimizer (Adam), and loss function (cross-entropy). In TTSNet, the network is trained in two stages. The CNN module is firstly trained for 300 epochs. The classification accuracy has converged within the number of training epochs. The model weight of the CNN module is then not updated in the following training process of the fully connected layer. In the training process of the second module, the Adam optimizer is additionally equipped with the weight decay (L2 penalty) of 0.1 to ensure the early stop of the training process.

3.2. Result

In this section, five methods are compared to the proposed TTSNet method, including FBTRCA, EEGNet, TEGNet, OTSNet and TTSSVM. EEG signals from Dataset I and Dataset II are used in three cases: (1) Dataset I(a)-Dataset I with the movement onset located, (2) Dataset I(b)-Dataset I without the located movement onset and (3) Dataset II without the located movement onset. In this section, we will used the dataset I(a) to analyze (1) the simplified network architecture in temporal decoding, (2) the influence of the temporal decoding and classifier, and (3) the necessity of the two-stage training process. The

overall performance of these methods in the three cases is compared finally.

Before the statistic analysis in the three cases, we first compare the EEG signals before and after spatial filtering (with task-related component analysis) in the channel space and the source space, which is given in Fig. 3. The figures for the channel space are plotted with EEGLab (Delorme and Makeig, 2004). The figures for the source space are plotted with Brainstorm (Tadel et al., 2011). During plotting the source space figures, the brain anatomy used is BCI-DNI BrainSuite (Joshi et al., 2022). The surface is segmented by the boundary element method with Brainstorm (Frijns et al., 2000). The source spaces figures are finally given by the standardized low-resolution brain electromagnetic tomography method (Pascual-Marqui, 2002).

3.2.1. Simplified neural network in temporal decoding

In TEGNet, the multi-channel EEG signals are first passed by a spatial filter, the filtered signals are then devoted into the EEGNet. Compared to EEGNet, the TEGNet reduces the dimension of EEG signals with a linear transform of size $C \times P$. This linear transform can be easily obtained by solving the Eigen equation in Eq. (3) with the training set. With the spatial filtering, the input of the neural network part in TEGNet has fewer number of channels. To show the equivalence of EEGNet and TEGNet, Fig. 4 compares the multi-class classification performance in the dataset I(a). The average classification accuracy is 0.4161 ± 0.0748 and 0.4205 ± 0.0776 on average for EEGNet and TEGNet, respectively.

3.2.2. Neural networks in temporal decoding and classifier

Before analyzing the temporal decoding, the role of the feature selection in FBTRCA must be clarified. In our previous work (Jia et al., 2023), we found that when the number of selected features is greater than a threshold after feature sorting, the classification accuracy has no significant differences from the case in which all the features are used. The feature selection in the multi-class FBTRCA serves for feature dimension reduction. In this work, to avoid the discussion on the number of selected features, we ignore the computation load and all the features are fed into the SVM classifier.

The TTSNet has two modifications on the FBTRCA method, including the EEGNet in the temporal decoding and the fully connected layer in the classification. Both modifications may lead changes to the classification performance. To check the influence of modified temporal decoding on the classification performance, the TTSSVM is compared to the proposed TTSNet. Ignoring the feature selection as mentioned above, the only difference between FBTRCA and TTSSVM is the temporal decoding part. The difference between TTSSVM and TTSNet is the classification part. Fig. 5 illustrates the classification comparison of FBTRCA, TTSSVM and TTSNet. It shows that the modifications in the temporal decoding and the classifier can increase the average classification accuracy with 1.92% and 2.03%, respectively. In total, TTSNet has an increase of 3.95% on the FBTRCA method.

3.2.3. Two-stage-training process

The training processing of parameters in the TTSNet adopts a two-stage process. In the first stage, the spatial filter is learned by solving the Eigen equation, and the parameters in EEGNets are learned with the filtered signals as inputs and the true labels as outputs. In the second stage, the learning of parameters in the EEGNet is turned off and the fully connected layer is trained. OTSNet holds the same structure as TTSNet but parameters in both EEGNet and fully connected layer are trained simultaneously. Fig. 6 compares the performance differences between OTSNet and TTSNet. The reason why TTSNet has a better performance than OSTNet is further explored in the discussion.
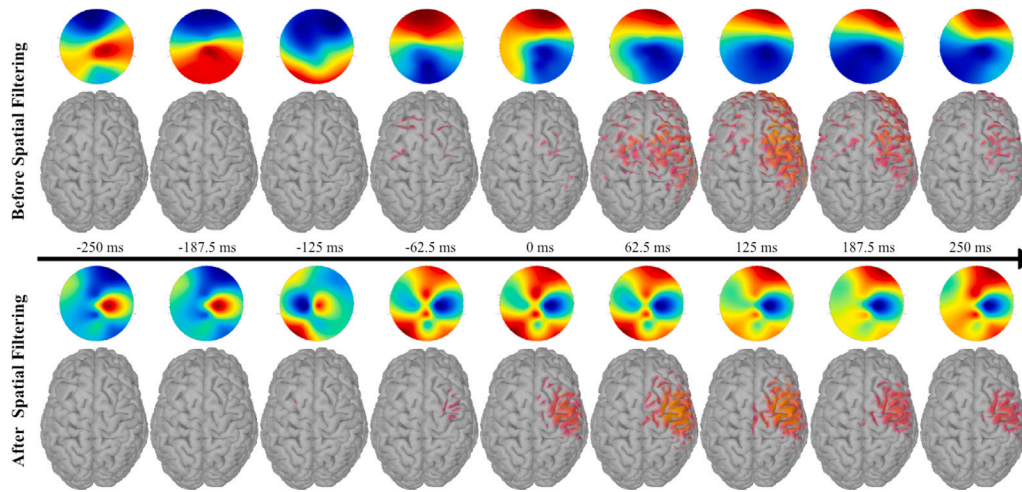
Fig. 3. Comparison of the grand average MRCP signals (0.5~10 Hz) before and after the spatial filtering. This figure visualizes the grand average MRCP signals of elbow flexion of subject 1 from dataset I in both the channel space and the source space. The 0 ms in the figure denotes the movement onset. When visualizing the signals after spatial filtering, the problem is that the number of channels of filtered signals is decreased. To solve this problem, the filtered signals $X^T W$ are multiplied by the inverse spatial filter W^T, and we get $X^T W W^T$. $X^T W W^T$ reserves the filtered signals to the original channels, whose number is the same as the channels before spatial filtering.
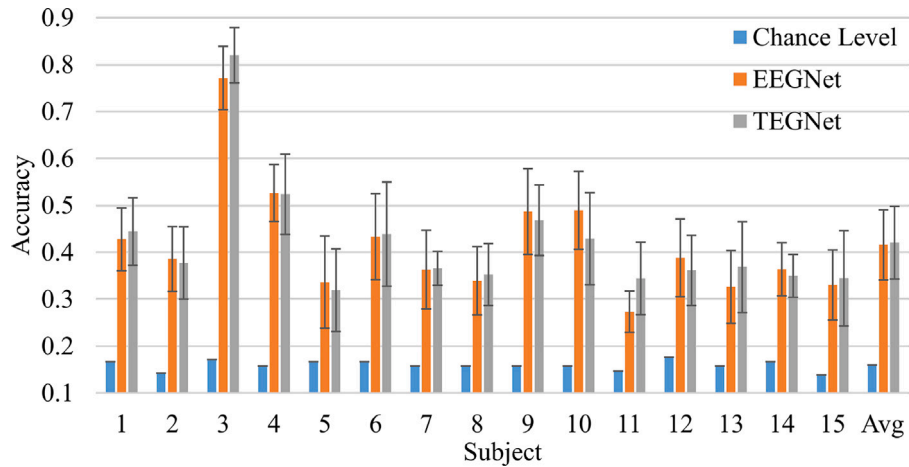

Fig. 4. Multi-class classification performance comparison between EEGNet and TEGNet, validated in dataset I(a). EEGNet and TEGNet have an equivalent performance in average.
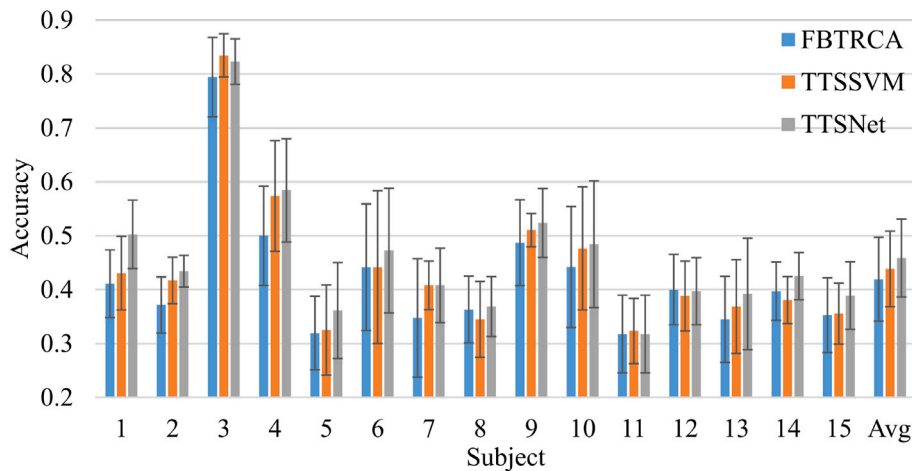

Fig. 5. Multi-class classification performance comparison among FBTRCA, TTSSVM and TTSNet.
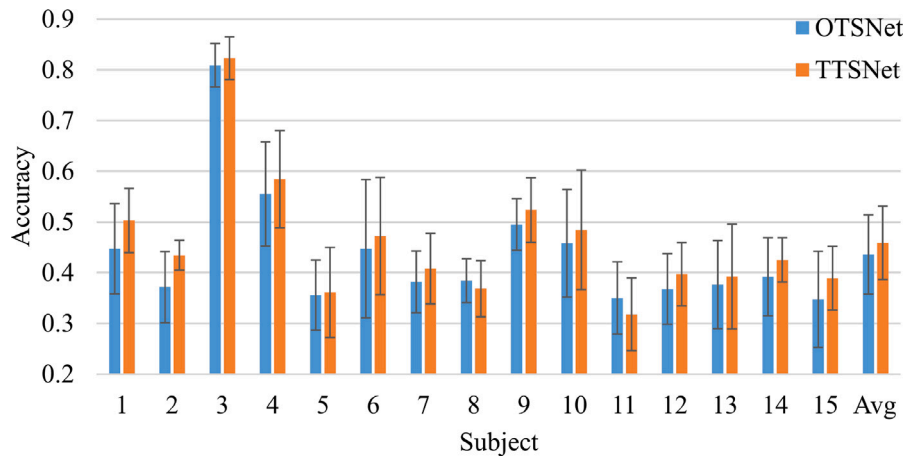
Fig. 6. Performance difference between the one-stage-training process and the two-stage-training process in the multi-class classification task.

Table 3
Overall average accuracy comparison.

Dataset	Dataset I(a)		Dataset I(b)		Dataset II	
	Binary	Multi-class	Binary	Multi-class	Binary	Multi-class
Chance level	0.5301 ± 0.0000	0.1594 ± 0.0000	0.5000 ± 0.0000	0.1429 ± 0.0000	0.5000 ± 0.0000	0.2000 ± 0.0000
FBTRCA	0.7487 ± 0.1250	0.4193 ± 0.0780	0.7414 ± 0.1258	0.3878 ± 0.0664	0.6647 ± 0.1190	0.3975 ± 0.0675
EEGNet	0.7340 ± 0.1246	0.4161 ± 0.0748	0.7246 ± 0.1161	0.3889 ± 0.0729	0.6718 ± 0.1160	0.4057 ± 0.0689
TEGNet	0.7176 ± 0.1252	0.4205 ± 0.0776	0.7126 ± 0.1189	0.3843 ± 0.0724	0.6627 ± 0.1148	0.3905 ± 0.0847
OTSNet	0.7521 ± 0.1211	0.4358 ± 0.0780	0.7375 ± 0.1171	0.3946 ± 0.0633	0.6857 ± 0.1135	0.4079 ± 0.0743
TTSSVM	0.7659 ± 0.1182	0.4385 ± 0.0702	0.7494 ± 0.1126	0.4017 ± 0.0633	0.7021 ± 0.1155	0.4121 ± 0.0736
TTSNet	**0.7707 ± 0.1168**	**0.4588 ± 0.0724**	**0.7526 ± 0.1122**	**0.4141 ± 0.0679**	**0.7075 ± 0.1159**	**0.4311 ± 0.0700**

Table 4
Two-sample t-test results: the *p*-values between TTSNet and the other methods in dataset I(a) are shown.

Subject	1	2	3	4	5	6	7	8
FBTRCA	0.0044	0.0038	0.3005	0.0604	0.2550	0.5650	0.1586	0.8434
EEGNet	0.0193	0.0556	0.0556	0.1243	0.5583	0.4159	0.2103	0.3306
TEGNet	0.0699	0.0421	0.9020	0.1536	0.3061	0.5191	0.1057	0.5693
OTSNet	0.1260	0.0175	0.4613	0.5229	0.8776	0.6636	0.3798	0.4872
	9	10	11	12	13	14	15	
	0.2687	0.4238	1.0000	0.9191	0.2666	0.2218	0.2380	
	0.3097	0.9095	0.1147	0.7911	0.1250	0.0141	0.0747	
	0.0934	0.2685	0.4377	0.2666	0.6035	0.0014	0.2546	
	0.2766	0.6061	0.3253	0.3332	0.7159	0.2482	0.2612	

3.3. Performance summary

In Table 3, the overall classification accuracies are listed, including binary and multi-class results in three dataset cases. Table 4 lists the *p*-values between TTSNet and the other methods in dataset I(a). The *p*-value is calculated using the two-sample t-test. The two sets of values passed to the two-sample t-test function are the ten values of the accuracy of the proposed TTSNet and the ten of the compared methods, respectively. In the dataset I(b) and the dataset II, the movement onset cannot be exactly located. The misalignment of the movement onset has a negative influence on the multi-class classification. The reason of the negative influence of the misalignment will be analyzed in the discussion. The TTSNet helps to improve the multi-class classification in dataset I(b). However, the classification performance in dataset I(b) still has a distance from the performance of dataset I(a). In summary, TTSNet contributes to the classification performance of FBTRCA by enhancing the temporal decoding process.

4. Discussion

In this work, our focus lies on the multi-class classification of single-side upper limb movements. We enhance the performance of our previously proposed FBTRCA method by introducing temporal decoding using a convolutional neural network. To underscore the contributions of this work, it is essential to discuss three key points: (1) the relationship between movements of the double-side and single-side of the limb, (2) the rationale for replacing correlation with a convolutional neural network, and (3) the novelty of the two-stage training process.

4.1. Single-side and double-side upper limb movement

The multi-class classification of limb movements involves two distinct tasks: (1) classification of multiple limbs and (2) classification of multiple movements on the same limb.

In the first task, classification methods are developed based on the brain phenomenon known as event-related desynchronization/synchronization (ERD/ERS). This phenomenon involves power changes on the brain scalp, with a decrease in power on the same side of the brain as the executing limb and an increase on the contra-side half of the brain. When different limbs execute movements, the activated brain regions vary accordingly. The spatial filter known as common spatial pattern (CSP) is employed in this task to distinguish the activated brain regions (Zhang et al., 2019). The classification methods for this task focus on power changes in multiple brain regions within the frequency range of 8 to 40 Hz.

Table 5
The difference between FBTRCA and FBCSP in limb movement classification.

Module	Task 1	Task 2
Task	Double-side Limb	single-side Limb
Brain activity	Motor imagery	movement-related cortical potential
Frequency range	8–40 Hz	0.5–10 Hz
Method	FBCSP (Ang et al., 2008)	FBTRCA (Jia et al., 2022, 2023)
Filter bank division	8–12 Hz, 12–16 Hz, …, 36–40 Hz	0.01–1 Hz, 0.01–2 Hz, …, 0.01–10 Hz
Spatial filter in each filter bank	Common spatial pattern	Task-related component analysis
Feature type in each filter bank	Log variances	Correlations
Feature fusion of all filter banks	Concatenation	
Feature selection method	Mutual-information based feature selection	

In the second task, an intuitive idea based on ERD/ERS is that power changes evoked by movements of the same limb are locate in the adjacent regions. Therefore, the classification of multiple movements on the same limb relies on the adjacent activated brain regions. In the adjacent brain regions, the spatial differences are more difficult to be distinguished than that in ERD/ERS. The temporal information are much more important for the single-side limb movements. In this task, the differences between classes are reflected in the grand average MRCPs of each class. After averaging the signals across trials, the signals are smoothed and limited to the frequency range of 0.5 to 10 Hz.

In both tasks, the filter-bank-based methods are used to extract and optimize the features, *i.e.* the FBTRCA in single-side limb and the filter bank CSP (FBCSP) in double-side limbs (Jia et al., 2022; Ang et al., 2008). The relationship between the two methods is shown in Table 5. The main difference between them is the feature types instead of the feature selection method.

In FBCSP, the log variances are computed from the non-overlapped narrow bands, indicating the powers in the narrow band. In some narrow bands, the power will change when carrying out motor imagination or execution. Compared to the narrow bands with unchanged powers, the narrow bands with changed powers are sparser. A more classical feature presentation is given in temporal-constraint sparse group spatial pattern (TCSGSP) (Zhang et al., 2019). In TCSGSP, based on the filter bank division in FBCSP, the filter banks are divided into multiple sliding time windows. For instance, the power keeps unchanged in the time window 0–1 s but it may change in the time window 1.25–2.25 s. Therefore, we think that the log variance features have a sparse representation in double-side limb movements. In other words, common spatial patterns are extracted from multiple frequency bands and sliding windows. The resulting features indicate differences ('1') or no differences ('0'), representing a sparse '0' and '1' problem. Feature selection in double-side limb movements focuses on selecting the '1' features against the '0' features.

In FBTRCA, the correlations are computed form the low-frequency bands. Note that the low cut-offs of these bands in Table 5 are fixed to a small value 0.5 Hz and the high cut-offs increase in an arithmetic sequence. In single-side limb movement, the main differences among classes are the signal trend and the trend is located in the low-frequency bands. Because the low-frequency bands are included in all filter banks, the accuracy of STRCA in these banks are close to each other but the best one is unknown. As explained in Jia et al. (2022), the best high cut-off for STRCA is difficult to locate due to the individual differences. FBTRCA is proposed to avoid the search of best high cut-off by combining all features from these filter banks. For instance, the classification accuracy of STRCA ranges from 0.85 to 0.95 across these filter banks. After concatenating the features of all filter banks, we have the features with the highest accuracy and we do not need to know to which filter bank it belongs. Because the number of features increases after concatenation, we used the mutual-information-based feature selection method, *i.e.* mRMR, to reduce the feature dimension for the final classification. In both FBTRCA and FBCSP, the feature selection method is used to reduce the increased feature dimension, which is induced by the concatenation step.

Compared to the sliding time window used in TCSGSP for double-side limb movements, it is difficult to apply the sliding window on

FBTRCA. The reason is that signal trend in MRCP is spread over the time dimension around the movement onset, instead of the sparse representation as in double-side limb movement. A more suitable approach is to adjust the weights applied to the signals in the correlation. In STRCA and FBTRCA, the weights are not trainable by parameter tuning.

4.2. From correlation to convolutional neural network

In our previously proposed STRCA method, both the spatial filter and the grand average MRCP were obtained from the training set. The grand average MRCP was computed by averaging EEG trials belonging to the same class in the training set. In the correlation features of an EEG trial, both the grand average MRCP and the EEG trial were first optimized with the spatial filter, and then the correlation between the EEG trial and the grand average MRCP was computed. The correlation value represented the sum of the weighted signals in the EEG trials, where the weights were determined by the grand average MRCP. Consequently, the grand average MRCP played a crucial role in extracting the correlation features. Averaging the signals in the grand average MRCP aimed to reduce the influence of noise in the original EEG trials. As illustrated in Fig. 7, the noise in the relatively high-frequency bands was effectively eliminated in the grand average MRCP.

However, the averaging operation can introduce inaccurate grand average MRCPs due to misalignment of movement onsets. To simplify the explanation of the misalignment problem, we made two assumptions. Firstly, we simplified the ideal curve of MRCP signals (an increase followed by a decrease) as a sine function. Secondly, we assumed that the noise in the EEG signals is uniformly distributed along the timeline and are fully eliminated by averaging.

In the training set of a class, two branches were assumed, each with an equal number of trials, and the noise was removed by averaging the trials within each branch. The movement onsets of trials within each branch were strongly aligned. However, the movement onsets between the two branches were not the same, and this was the only difference between them. After averaging the trials within each branch, Fig. 8(a) illustrates the latency lag between the two branches. Considering that both branches belong to the training set, the final grand average MRCP is obtained by averaging the MRCPs from the two branches. However, the latency lag between the two branches can influence the shape of the grand average MRCP, as shown in Fig. 8(b). The latency lag distorts the shape of the grand average MRCP in two ways: by reducing the highest amplitude/power and by introducing bias in the timing.

In the computation of the real grand average MRCP, the situation becomes more complex as the movement onsets of all trials may not be the same, unlike the two distinct movement onsets illustrated in Fig. 8. In cases where the movement trajectory is available, such as in dataset I(a), the movement onsets can be localized, and the EEG signals before and after the movement onset can be sliced for the classification task. By individually locating the movement onsets for all trials, the latency lag depicted in Fig. 8(a) can be minimized. However, in most cases, the movement trajectories are not recorded simultaneously, and the EEG signals are typically sliced from the two-second time window after the cue to execute the movement. Due to variations in the reflection time from the brain to the limb, the distance between the movement
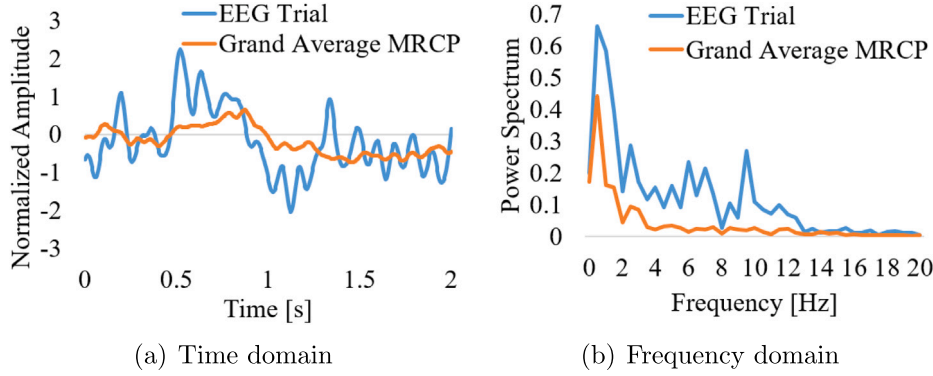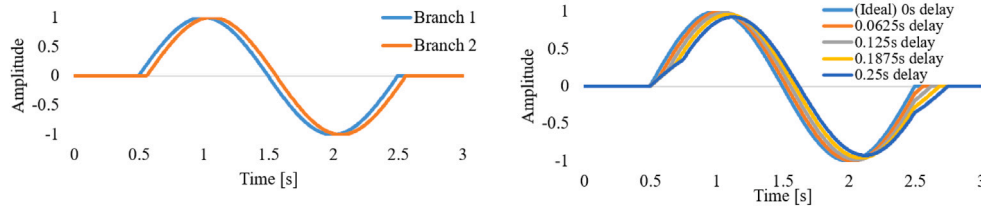
(a) Time domain

(b) Frequency domain

Fig. 7. The difference between the grand average MRCP and an EEG trial. This figure is an example whose data is extracted from the channel C_z of the *elbow flexion*.

(a) The grand average MRCP of two branches. Noise is fully removed after averaging. There is a lag off between the movement onsets of trials in two branches.

(b) In the grand average MRCP of the training set, the grand average MRCP of two branches are averaged. The lag off between two branches leads to the distortion of the grand average MRCP.

Fig. 8. Influences of misaligned movement onset on the grand average MRCP. The ideal grand average MRCP is simplified into a sine wave and noise is diminished to zeros after averaging across trials. The training set consists of two branches and two branches have the same number of trials.

onset and the cue to execute the movement differs across trials, and this cannot be precisely measured. Consequently, this leads to distortions in the ideal grand average MRCP, as shown in Fig. 8(b).

Although the movement onset in dataset I(a) can be localized with the movement trajectory, we acknowledge the possibility of misalignment caused by the inaccurate localization of the onset and the unmeasurable reflection time from the brain to the limb. To mitigate the influence of the distorted grand average MRCP on feature extraction, we propose replacing this weight (the grand average MRCP) with a more trainable weight (EEGNet).

4.3. Two-stage-training process

In the proposed TTSNet method, two modifications are applied to the previous FBTRCA method: the utilization of EEGNet in the temporal decoding and the incorporation of fully connected layers in the classification. During the training of TTSNet, the parameters of the EEGNet and the fully connected layer are trained in two separate steps. This two-stage training process is implemented to fulfill the requirements of the filter bank technique in MRCP signal processing.

The two-step-training process is motivated by FBTRCA. Two points must be emphasized during the development of the two-stage-training process.

The first point is that the STRCA is used to extract the features from a single filter bank. The correlation features in STRCA can be used to predict the classes with signals in the single filter bank. When changing from the correlation to convolution, the STRCA is replaced with the TEGNet (Task-related component analysis + EEGNet). The TEGNet is supposed to be able to predict the classes within the filter bank as well. Therefore, in the first stage, we need to ensure the TEGNet are trained and fully converged.

The second point is that the feature selection method is used to optimize the feature dimension after the feature concatenation. In the TTSSVM, the followed SVM classifier is used to predict the classes. In the TTSNet, the fully connected layer is used to reduce the feature dimension and predict the classes. Without ignoring the feature selection, it is difficult to decide on how many features should be fed into SVM, because the number of features in FBTRCA and TTSNet are not the same after the feature extraction from multiple bands. The number of features is $3KF$ in FBTRCA and the number of features is KF in TTSNet, where K is the number of classes and F is the number of filter banks. Because the feature selection process in FBTRCA is to reduce the feature dimension but has a low improvement on the classification accuracy, we simply ignore the feature selection process in the two-stage process.

4.4. Reasons to develop single-side limb movements

The development and application in identifying single-side limb movements and supporting the rehabilitation of stroke patients hold significant implications and potential consequences. In the traditional BCI applications, the control commands are mainly generated based on the visual-evoked potential and double-side limb movements. Compared to the visual-evoked potential, brain activities evoked by limb movements are more natural for the stroke patients to generate control commands because we are used to interact with the external environment by limb movement. The breakthrough in the single-side limb movement enriches the interaction approaches between the brain and the environment, and thus help to assist the rehabilitation of the stroke.

5. Conclusion

In this work, we propose TTSNet, a method that leverages both temporal and spectral information to decode patterns from MRCP

signals. TTSNet integrates the temporal decoding capability of EEGNet into the FBTRCA method, enabling the extraction of distinct features that capture both temporal and spectral characteristics. This method is applicable to both binary and multi-class classification tasks for upper limb movements. Our results demonstrate that TTSNet outperforms both FBTRCA and EEGNet in decoding pre-movement patterns. The findings of this study have implications for the rehabilitation of individuals with disabled or weak upper limbs. The code repository for this work can be accessed via the following link: https://github.com/plustar/Movement-Related-Cortical-Potential.git.

CRediT authorship contribution statement

Hao Jia: Conceptualization, Methodology, Visualization, Data curation, Formal analysis, Investigation, Software, Writing – original draft, Writing – review & editing. **Shuning Han:** Data curation, Visualization, Formal analysis, Software, Writing – review & editing. **Cesar F. Caiafa:** Supervision, Visualization, Conceptualization, Methodology, Resources, Writing – review & editing. **Feng Duan:** Writing – review & editing, Visualization, Project administration, Resources, Supervision. **Yu Zhang:** Conceptualization, Resources, Validation, Writing – review & editing. **Zhe Sun:** Conceptualization, Methodology, Resources, Validation, Writing – review & editing. **Jordi Solé-Casals:** Conceptualization, Methodology, Resources, Supervision, Validation, Visualization, Writing – review & editing.

Declaration of competing interest

The authors declare that they have no known competing financial interests or personal relationships that could have appeared to influence the work reported in this paper.

Data availability

The data used in this work are already publicly available.

Acknowledgments

Statement: During the preparation of this work the author(s) used Pytorch in order to generate neural network models. After using this tool/service, the author(s) reviewed and edited the content as needed and take(s) full responsibility for the content of the publication.

References

Ang, K.K., Chin, Z.Y., Zhang, H., Guan, C., 2008. Filter bank common spatial pattern (FBCSP) in brain-computer interface. In: 2008 IEEE International Joint Conference on Neural Networks (IEEE World Congress on Computational Intelligence). IEEE, pp. 2390–2397. http://dx.doi.org/10.1109/IJCNN.2008.4634130, URL: http://ieeexplore.ieee.org/document/4634130/. event-place: Hong Kong, China.

Barachant, A., Bonnet, S., Congedo, M., Jutten, C., 2012. Multiclass brain–computer interface classification by Riemannian geometry. IEEE Trans. Biomed. Eng. 59 (4), 920–928. http://dx.doi.org/10.1109/TBME.2011.2172210, URL: http://ieeexplore.ieee.org/document/6046114/.

Borràs, M., Romero, S., Alonso, J.F., Bachiller, A., Serna, L.Y., Migliorelli, C., Mañanas, M.A., 2022. Influence of the number of trials on evoked motor cortical activity in EEG recordings. J. Neural Eng. 19 (4), 046050. http://dx.doi.org/10.1088/1741-2552/ac86f5, URL: https://iopscience.iop.org/article/10.1088/1741-2552/ac86f5.

Delorme, A., Makeig, S., 2004. EEGLAB: An open source toolbox for analysis of single-trial EEG dynamics including independent component analysis. J. Neurosci. Methods 134 (1), 9–21. http://dx.doi.org/10.1016/j.jneumeth.2003.10.009, URL: https://linkinghub.elsevier.com/retrieve/pii/S0165027003003479.

Duan, F., Jia, H., Sun, Z., Zhang, K., Dai, Y., Zhang, Y., 2021. Decoding premovement patterns with task-related component analysis. Cogn. Comput. 13 (5), 1389–1405. http://dx.doi.org/10.1007/s12559-021-09941-7, URL: https://link.springer.com/10.1007/s12559-021-09941-7.

Edelman, B.J., Baxter, B., He, B., 2016. EEG source imaging enhances the decoding of complex right-hand motor imagery tasks. IEEE Trans. Biomed. Eng. 63 (1), 4–14. http://dx.doi.org/10.1109/TBME.2015.2467312, URL: http://ieeexplore.ieee.org/document/7192613/.

Farina, D., Jensen, W., Akay, M. (Eds.), 2013. Introduction to Neural Engineering for Motor Rehabilitation. John Wiley & Sons, Hoboken, N.J.

Frijns, J., de Snoo, S., Schoonhoven, R., 2000. Improving the accuracy of the boundary element method by the use of second-order interpolation functions [EEG modeling application]. IEEE Trans. Biomed. Eng. 47 (10), 1336–1346. http://dx.doi.org/10.1109/10.871407, URL: http://ieeexplore.ieee.org/document/871407/.

Ghani, U., Jochumsen, M., Gyldenvang, M.B., Niazi, I.K., 2023. Can water-based EEG caps record robust movement-related cortical potentials (MRCPs) for single and multiple joint movements? In: 2023 45th Annual International Conference of the IEEE Engineering in Medicine & Biology Society. EMBC, pp. 1–4. http://dx.doi.org/10.1109/EMBC40787.2023.10340665.

Grosse-Wentrup, M., Buss, M., 2008. Multiclass common spatial patterns and information theoretic feature extraction. IEEE Trans. Biomed. Eng. 55 (8), 1991–2000. http://dx.doi.org/10.1109/TBME.2008.921154, URL: https://ieeexplore.ieee.org/document/4473042/.

Hramov, A.E., Maksimenko, V.A., Pisarchik, A.N., 2021. Physical principles of brain–computer interfaces and their applications for rehabilitation, robotics and control of human brain states. Phys. Rep. 918, 1–133. http://dx.doi.org/10.1016/j.physrep.2021.03.002, URL: https://linkinghub.elsevier.com/retrieve/pii/S0370157321001095.

Jeong, J.-H., Kwak, N.-S., Guan, C., Lee, S.-W., 2020. Decoding movement-related cortical potentials based on subject-dependent and section-wise spectral filtering. IEEE Trans. Neural Syst. Rehabil. Eng. 28 (3), 687–698. http://dx.doi.org/10.1109/TNSRE.2020.2966826, URL: https://ieeexplore.ieee.org/document/8960436/.

Jia, H., Feng, F., Caiafa, C.F., Duan, F., Zhang, Y., Sun, Z., Solé-Casals, J., 2023. Multi-class classification of upper limb movements with filter bank task-related component analysis. IEEE J. Biomed. Health Inf. 1–11. http://dx.doi.org/10.1109/JBHI.2023.3278747, URL: https://ieeexplore.ieee.org/document/10135081/.

Jia, H., Sun, Z., Duan, F., Zhang, Y., Caiafa, C.F., Solé-Casals, J., 2022. Improving pre-movement pattern detection with filter bank selection. J. Neural Eng. http://dx.doi.org/10.1088/1741-2552/ac9e75, URL: http://iopscience.iop.org/article/10.1088/1741-2552/ac9e75.

Joshi, A.A., Choi, S., Liu, Y., Chong, M., Sonkar, G., Gonzalez-Martinez, J., Nair, D., Wisnowski, J.L., Haldar, J.P., Shattuck, D.W., Damasio, H., Leahy, R.M., 2022. A hybrid high-resolution anatomical MRI atlas with sub-parcellation of cortical gyri using resting fMRI. J. Neurosci. Methods 374, 109566. http://dx.doi.org/10.1016/j.jneumeth.2022.109566, URL: https://linkinghub.elsevier.com/retrieve/pii/S0165027022000930.

Kaeseler, R.L., Johansson, T.W., Struijk, L.N.S.A., Jochumsen, M., 2022. Feature and classification analysis for detection and classification of tongue movements from single-trial pre-movement EEG. IEEE Trans. Neural Syst. Rehabil. Eng. 30, 678–687. http://dx.doi.org/10.1109/TNSRE.2022.3157959, URL: https://ieeexplore.ieee.org/document/9734730/.

Kawala-Sterniuk, A., Browarska, N., Al-Bakri, A., Pelc, M., Zygarlicki, J., Sidikova, M., Martinek, R., Gorzelanczyk, E.J., 2021. Summary of over fifty years with brain-computer interfaces—A review. Brain Sci. 11 (1), 43. http://dx.doi.org/10.3390/brainsci11010043, URL: https://www.mdpi.com/2076-3425/11/1/43.

Lawhern, V.J., Solon, A.J., Waytowich, N.R., Gordon, S.M., Hung, C.P., Lance, B.J., 2018. EEGNet: A compact convolutional network for EEG-based brain-computer interfaces. J. Neural Eng. 15 (5), 056013. http://dx.doi.org/10.1088/1741-2552/aace8c, URL: http://arxiv.org/abs/1611.08024.

Liu, C., You, J., Wang, K., Zhang, S., Huang, Y., Xu, M., Ming, D., 2023. Decoding the EEG patterns induced by sequential finger movement for brain-computer interfaces. Front. Neurosci. 17, http://dx.doi.org/10.3389/fnins.2023.1180471, URL: https://www.frontiersin.org/journals/neuroscience/articles/10.3389/fnins.2023.1180471.

Ofner, P., Schwarz, A., Pereira, J., Müller-Putz, G.R., 2017. Upper limb movements can be decoded from the time-domain of low-frequency EEG. PLOS ONE 12 (8), e0182578. http://dx.doi.org/10.1371/journal.pone.0182578, URL: https://dx.plos.org/10.1371/journal.pone.0182578.

Ofner, P., Schwarz, A., Pereira, J., Wyss, D., Wildburger, R., Müller-Putz, G.R., 2019. Attempted arm and hand movements can be decoded from low-frequency EEG from persons with spinal cord injury. Sci. Rep. 9 (1), 7134. http://dx.doi.org/10.1038/s41598-019-43594-9, URL: http://www.nature.com/articles/s41598-019-43594-9.

Olsen, S., Signal, N., Niazi, I.K., Christensen, T., Jochumsen, M., Taylor, D., 2018. Paired associative stimulation delivered by pairing movement-related cortical potentials with peripheral electrical stimulation: An investigation of the duration of neuromodulatory effects: PAS via pairing MRCPs with electrical stimulation. Neuromodulation: Technol. Neural Interface 21 (4), 362–367. http://dx.doi.org/10.1111/ner.12616, URL: http://doi.wiley.com/10.1111/ner.12616.

Pascual-Marqui, R.D., 2002. Standardized low-resolution brain electromagnetic tomography (sLORETA): technical details. Clin. Pharmacol. 16.

Saha, S., Mamun, K.A., Ahmed, K., Mostafa, R., Naik, G.R., Darvishi, S., Khandoker, A.H., Baumert, M., 2021. Progress in brain computer interface: Challenges and opportunities. Front. Syst. Neurosci. 15, 578875. http://dx.doi.org/10.3389/fnsys.2021.578875, URL: https://www.frontiersin.org/articles/10.3389/fnsys.2021.578875/full.

Sburlea, A.I., Montesano, L., Minguez, J., 2015. Continuous detection of the self-initiated walking pre-movement state from EEG correlates without session-to-session recalibration. J. Neural Eng. 12 (3), 036007. http://dx.doi.org/10.1088/1741-2560/12/3/036007.

Schirrmeister, R.T., Springenberg, J.T., Fiederer, L.D.J., Glasstetter, M., Eggensperger, K., Tangermann, M., Hutter, F., Burgard, W., Ball, T., 2017. Deep learning with convolutional neural networks for EEG decoding and visualization: Convolutional neural networks in EEG analysis. Hum. Brain Mapp. 38 (11), 5391–5420. http://dx.doi.org/10.1002/hbm.23730, URL: https://onlinelibrary.wiley.com/doi/10.1002/hbm.23730.

Tadel, F., Baillet, S., Mosher, J.C., Pantazis, D., Leahy, R.M., 2011. Brainstorm: A user-friendly application for MEG/EEG analysis. Comput. Intell. Neurosci. 2011, 1–13. http://dx.doi.org/10.1155/2011/879716, URL: http://www.hindawi.com/journals/cin/2011/879716/.

Thuwajit, P., Rangpong, P., Sawangjai, P., Autthasan, P., Chaisaen, R., Banluesombatkul, N., Boonchit, P., Tatsaringkansakul, N., Sudhawiyangkul, T., Wilaiprasitporn, T., 2022. EEGWaveNet: Multiscale CNN-based spatiotemporal feature extraction for EEG seizure detection. IEEE Trans. Ind. Inform. 18 (8), 5547–5557. http://dx.doi.org/10.1109/TII.2021.3133307, URL: https://ieeexplore.ieee.org/document/9645336/.

Zhang, Y., Nam, C.S., Zhou, G., Jin, J., Wang, X., Cichocki, A., 2019. Temporally constrained sparse group spatial patterns for motor imagery BCI. IEEE Trans. Cybern. 49 (9), 3322–3332. http://dx.doi.org/10.1109/TCYB.2018.2841847, URL: https://ieeexplore.ieee.org/document/8386437/.